J. Membrane Biol. 148, 99–110 (1995)

The Journal of
Membrane
Biology

Topical Review

Optical Methods to Measure Membrane Transport Processes

A.S. Verkman
Departments of Medicine and Physiology, Cardiovascular Research Institute, University of California, San Francisco, CA 94143-0521

Received: 12 April 1995/Revised: 9 June 1995

Introduction

Cell viability requires the constitutive and regulated transport of various neutral and charged molecules across biological membranes (membrane transport). Solute transport across cell plasma membranes serves many functions, including the accumulation and excretion of metabolites, the maintenance of intracellular ionic composition, and the regulation of intracellular pH and volume. In epithelia, a polarized distribution of plasma membrane transporters facilitates the vectorial movement of water and solutes across a cell layer; in electrically excitable cells of the neuromuscular system, voltage-dependent ion channels generate propagating electrical signals. Membrane transport is also essential for the functioning of intracellular membranes, including mitochondrial energy transduction, maintenance of acidity in the endosomal and secretory compartments, and regulation of the intranuclear milieu.

Membrane transport proteins have been classified based on inferred mechanisms of transport. The term "active transporter" refers to a protein which utilizes the energy provided by ATP hydrolysis to transport solutes against electrochemical gradients. Examples of active transporters (or "pumps" or "ATPases") are the $3Na^+/2K^+$ pump, H^+ pump, H^+/K^+ pump and Ca^{++} pump. The term "secondary active transporter" refers to non-ATP-coupled proteins which utilize the electrochemical gradients produced by active transporters. This terminology is often confusing and probably should be replaced with the term "passive transporter." Of the passive transporters, an historical distinction has been made between "channels" and "carriers." The term *channel* (e.g., Na^+, K^+, Cl^-, Ca^{++} channel) generally refers to a gated conductive transporter with high turnover rate, possibly involving ion movement through an aqueous pore. The term *carrier* implies slower transporting rates involving distinct substrate-transporter binding/unbinding events and conformational changes. Classical carriers include the band 3 Cl^-/HCO_3^- exchanger, Na^+/H^+ antiporter and $Na^+/K^+/2Cl^-$ cotransporter. It is less certain with this system how to classify transporters for water, urea and glucose. The distinction between channels *vs.* carriers has become outdated with the molecular cloning of various transporting proteins and soon the elucidation of transport protein structure and transporting mechanisms.

The membrane transport problem is to quantify the transport of a solute across a rate-limiting barrier separating two well-stirred compartments in response to a defined electrochemical driving force. The barrier may consist of a single membrane, a single cell layer (epithelium), or a multicell layer. Transport measurements provide fundamental information about the physiological functions of epithelia, cells, and subcellular organelles. In addition, transport measurements have distinct purposes prior to, during and after transporter cloning. Precloning transport measurements provide evidence for the existence of a facilitated solute pathway, furnish empirical permeability parameters such as permeability coefficients and solute affinities, and facilitate transporter purification. Transport measurements may permit the expression cloning of transporter cDNAs, and are required for functional characterization of putative cDNA clones. Postcloning transport measurements enable the identification of disease-related mutations, and with mutagenesis, the examination of transporting mechanisms.

Key words: Fluorescence — Membrane permeability — Water transport — Ion transport — Light scattering — Membrane potential

Correspondence to: A.S. Verkman

This review is focused on optical methods to measure membrane transport processes. Optical methods often have remarkable advantages over alternative approaches such as radiolabeled solutes. Optical methods permit the real-time study of very small or heterogeneous samples (single cells or small amounts of reconstituted proteoliposomes) with high accuracy, and the measurement of rapid transport processes in which labeled solute and membrane cannot be physically separated. The general strategy is to identify a measurable optical parameter, such as the intensity of scattered light or the fluorescence of an entrapped indicator, which is sensitive to the transport event of interest (e.g., Cl^- movement across a liposome membrane). The optical signal must be sensitive and selective for the transport event, have a rapid response rate, and produce minimal perturbation of normal membrane function. After establishing a quantitative relationship between optical signal and the transport event (e.g., fluorescence intensity *vs.* intraliposomal Cl^- activity), transport rates can be measured in response to defined electrochemical driving forces, and putative transport inhibitors and activators can be tested.

The purpose of this review is to provide the reader with practical information about modern optical methods available to measure membrane transport processes. A limited amount of technical information is provided to evaluate the feasibility and limitations of alternative optical techniques to a given problem. Because of space limitations, the cited references have been chosen primarily for their inclusion of methodological developments and technical details.

Water Transport and Volume Measurements

Osmotic Water Permeability

Osmotic water transport is the net flow of volume across a membrane in response to a hydrostatic or osmotic driving force,

$$J_v = P_f S V_w[(P_1 - P_2)/RT + \Sigma\sigma_i(\Pi_{2i} - \Pi_{1i})] \quad (1)$$

where J_v is volume flow (cm^3/sec) from compartment 1 to 2, P_f is the osmotic water permeability coefficient (cm/sec), S is surface area (cm^2), V_w is the partial molar volume of water (cm^3/mol), P is hydrostatic pressure (atm), σ_i is the reflection coefficient of the ith solute, and Π_i the osmolality of the ith solute (mOsm). A high P_f (generally >0.01 cm/sec) provides evidence for the presence of molecular water channels. For most biological situations, the hydrostatic term is small and $\sigma_i \sim 1$. The reader is referred to several reviews for details about the biophysics of water permeability [3, 25, 73, 75].

The measurement of water transport is thus a problem of volume or volume flow determination. Measurement of P_f has become increasingly important with the recent identification of a family of water transporting proteins (aquaporins) expressed in various mammalian tissues [1, 75]. In addition, volume measurements have applications in the study of cell volume regulation, epithelial fluid absorption/secretion, and solute transport (*see below*), provided that osmotic gradients are established as a consequence of solute transport. A variety of optical methods are available to measure water transport in small vesicles, cells and epithelia, all based on the changes in volume which accompany osmotic water movement.

Water Transport in Vesicles: Light Scattering

The light-scattering method provides a rapid and direct approach to measure osmotic water permeability in osmotically responsive, sealed membrane vesicles and some small cells. Light scattering was developed initially for water permeability measurements in erythrocytes, and subsequently applied to membrane vesicles, liposomes reconstituted with water channels and cell suspensions [70, 73]. The method is based on the dependence of elastically scattered light (Rayleigh scattering) on vesicle volume. Experimentally, a vesicle suspension is mixed rapidly with an anisosmotic solution (generally hypertonic) to generate a transmembrane osmotic gradient. Mixing is usually accomplished by a stopped-flow apparatus in which small volumes (0.02–0.1 ml) of two solutions are mixed together in <1 msec. As osmotic water flux occurs, the time course of scattered light intensity provides an instantaneous measure of vesicle volume (Fig. 1*A*). Curve-fitting procedures have been developed to determine P_f from the light-scattering time course, vesicle size, and the calibration relation between light scattering and vesicle volume [79]. The light scattering method is simple to apply and very small samples are required; however, there are potential problems in quantitative data interpretation, including cell/vesicle size heterogeneity, motion artifacts just after mixing which occur before flow stops, refractive index changes which produce anomalous scattering signals, and in cells, scattering from intracellular structures [18, 47].

Water Transport in Vesicles: Fluorescence Quenching

Many fluorophores with overlapping fluorescence excitation and emission spectra undergo "fluorescence self-quenching"; as fluorophore concentration increases, fluorescence intensity decreases by a nonradiative energy transfer mechanism. To exploit self-quenching for measurement of volume, vesicles loaded with a high concentration of fluorophore are subjected to an inwardly directed osmotic gradient in a stopped-flow apparatus [17].

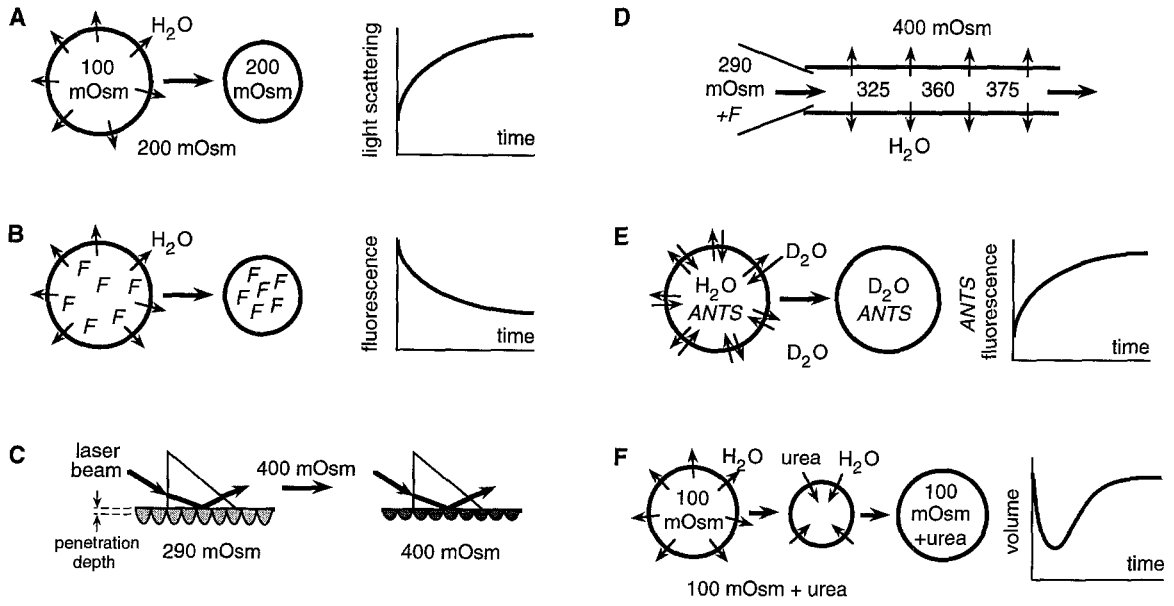

Fig. 1. Experimental strategies to measure water and solute transport. (*A*) Light-scattering measurement of osmotic water permeability. Vesicles are subjected to an inwardly directed osmotic gradient (100 mOsm inside, 200 mOsm outside) causing shrinkage and increased 90° light scattering. (*B*) Fluorescence-quenching measurement of osmotic water permeability. Cells loaded with a dye (*F*) that undergoes fluorescence self-quenching are subjected to an osmotic gradient. As the vesicle shrinks, the concentrated fluorophore is self-quenched and fluorescence decreases. (*C*) Measurement of osmotic water permeability in adherent cells by total internal reflection fluorescence. Cells are loaded with a membrane impermeant volume marker. A thin (50–200 nm) layer of cytosol (labeled "penetration depth") is illuminated by a laser beam directed through a glass prism at a subcritical illumination angle. As the cell shrinks in response to an osmotic gradient (400 mOsm bathing solution), fluorophore concentration in the illuminated region increases. (*D*) Osmotic water permeability in a perfused tubular epithelium measured by a luminal fluorophore. An isolated tubule is perfused with an iso-osmolar solution (290 mOsm) containing a membrane-impermeant fluorescent marker (*F*) and bathed in a hyperosmolar solution (400 mOsm). As solute-free water is extracted from the tubule lumen, both luminal osmolality (values shown) and the concentration of *F* increase. (*E*) Diffusional water permeability measured by ANTS fluorescence. Vesicles loaded with ANTS in an H_2O buffer are mixed with an iso-osmolar D_2O buffer. As H_2O exchanges for D_2O, ANTS fluorescence increases. (*F*) Urea permeability measured by vesicle volume changes. Vesicles are subjected to an inward gradient of urea. Because permeability of water is faster than that of urea, there is initial osmotic efflux followed by urea and water influx, returning volume to its initial level. *See* text for details.

Osmotic water efflux produces increased intravesicular fluorophore concentration, resulting in instantaneous self-quenching and decreased fluorescence (Fig. 1*B*). Carboxyfluorescein and calcein are useful fluorophores for these studies. P_f is determined from the fluorescence time course, vesicle size, and the calibration of fluorescence *vs.* size. In contrast to light-scattering methods, the fluorescence signal is not sensitive to mixing and refractive index artifacts. Fluorescence-quenching has been used to measure water permeability in plasma membrane vesicles [17] and endosomes from kidney [80] and toad urinary bladder [36, 67], where labeling was accomplished in intact cells or organs by fluid-phase endocytosis of the fluorescent probe.

Water Permeability in Cell Plasma Membranes

Light scattering methods are potentially useful for volume measurements in suspended cells. Measurement of water permeability in single adherent cells in culture (or after immobilization on a coverglass by polylysine) is often required in polarized epithelial cells or when cell heterogeneity exists because of multiple cell types in a primary culture, or variable expression in a transient transfection system. As in vesicle studies, the experimental protocol is to measure the time course of scattered light intensity in response to a rapid change in extracellular solution osmolality. Rapid exchange (<50 msec) of perfusion solutions can be accomplished by a laminar flow channel design [22]. Several approaches are potentially useful to measure cell volume. For some cells with favorable geometry (e.g., well-separated dome shape), light scattering provides a volume-dependent optical signal [22, 26]. However, the signals are generally small, sensitive to nonvolume factors including solution refractive index and cell geometry, and not easily amenable to quantitative P_f determination.

Several approaches that utilize fluorescence detection have been described based on the change in the concentration of a membrane-impermeable fluorescent probe, such as calcein or BCECF, that accompanies changes in cell volume. Semiquantitative information about fluorophore concentration can be obtained by sam-

pling a thin (~1 μm) slice of cytosol by confocal microscopy. Alternately, partial confocal behavior can be conferred to a conventional epifluorescence microscope by use of a high numerical aperture objective and positioning of an aperture in the back focal image plane [56]. A general quantitative approach to measurement of relative cell volume in adherent cell monolayers involves fluorescence excitation by total internal reflection fluorescence (TIRF). TIRF involves the excitation of fluorophores in membrane-adjacent cytosol near a high-to-low refractive index interface produced by a glass-water boundary [6] (Fig. 1*C*). As cell volume decreases, the cytosolic fluorophore becomes concentrated and the fluorescence signal increases. Because the effective depth of TIR illumination (25–200 nm) is much smaller than cell thickness (and much smaller than possible by confocal microscopy), TIRF provides a quantitative and relatively simple approach to monitor relative cell volume in adherent cells of arbitrary shape and size [24]. In addition, fluorophore photobleaching is minimal in TIRF because a small fraction of total cell volume is illuminated.

Two relatively technically demanding approaches to measure cell volume should be mentioned. Reconstructions of cell shape by analysis of differential interference contrast [28] or fluorescence confocal images [24] can provide information about absolute cell volume; however, technical limitations in data acquisition and analysis make real-time volume measurements very difficult. A novel method to measure changes in the relative volume of single cells was developed recently based on 3-dimensional single particle tracking [39]. Fluorescently-labeled polystyrene beads are immobilized on the cell surface and the vertical (z-axis) position of a single bead is followed in response to changes in perfusate osmolality. Image analysis utilizing astigmatic detection optics permits measurement of bead z-position to ~10 nm accuracy with ~5 Hz sampling frequency.

An important application of cell volume measurement is the study of water permeability in *Xenopus* oocytes (~1.2 mm diameter spheres) transfected with putative water channel cDNAs. Because of mechanical limitations in oocyte swelling, better than 0.1% accuracy in volume measurement with 1-sec time resolution is required. The original swelling assay involved dilution of the extracellular solution with distilled water, and estimation of oocyte volume by measurement of two orthogonal oocyte diameters on a video monitor every 1–5 min [27]. An improved quantitative imaging approach was subsequently developed in which the shadow cast by an oocyte was recorded and digitized using transmission light microscopy [87]. Relative oocyte volume was computed rapidly from cross-sectional area (assumed to be proportional to $[\text{volume}]^{2/3}$) by pixel summation. This approach has been utilized extensively to study new water channel cDNAs and to test whether various transporting proteins contain aqueous pores [76].

Water Transport Across Epithelia

The water permeability measurements described above rely on transient measurements of vesicle or cell volume changes. Determination of epithelial water transport generally involves the steady-state measurement of net volume flow across an epithelial layer in response to a continuously imposed osmotic gradient. For a flat epithelial sheet, as would be mounted in an Ussing chamber, there is no good optical approach to quantify transepithelial water permeability; the most accurate approach to measure net volume movement remains capacitance probe and related techniques [37]. For small tubelike epithelial layers, such as kidney tubules and airways, the conventional approach to measure P_f has been the timed collection of fluid perfused through the tubule lumen. An impermeable tracer (e.g., ^{3}H-inulin) is perfused through the lumen and a transepithelial osmotic gradient is established by bathing the tubule in hypo-osmotic or hyperosmotic solutions. For a hyperosmotic bathing solution, solute-free water is extracted along the length of the tubule and the tracer concentration increases (Fig. 1*D*). P_f is calculated from the tracer concentration, lumen flow, lumen and bath osmolalities, and tubule length and surface area [2]. A simple fluorescence method relies on the replacement of the radiotracer by a membrane-impermeant fluorescent indicator [44]. The change in fluorophore concentration, determined from the luminal fluorescence of a distal segment of tubule, provides a quantitative measure of P_f. This approach was used to determine the kinetics of vasopressin-induced turn-on and turn-off of P_f in kidney collecting duct and the influence of transcellular volume flow on rates of endosomal trafficking [45].

Diffusional Water Permeability

A second parameter describing water movement is the diffusional water permeability coefficient P_d (cm/sec). The diffusional water permeability of a membrane is defined as transport of tracer-labeled water between compartments in the absence of an osmotic gradient, $P_d = J_d/S([^*H_2O]_1 - [^*H_2O]_2)$, where J_d is the flux of labeled water and $[^*H_2O]$ is the concentration of labeled water. Although P_d is not a physiologically important parameter, it provides important information about the nature of the water-transporting pathway. The ratio P_f/P_d is unity for water movement across a simple bilayer, and greater than unity for water movement through a wide pore or narrow channel [25, 75] (or when P_d is artifactually low because of unstirred layers, *ref.* 5).

Conventional (nonoptical) strategies to measure P_d

rely on use of radioactively (^3H_2O) or magnetically (NMR) labeled water [12, 73]. Measurement of ^3H_2O uptake is very challenging because of rapid water diffusional transport rates, and NMR requires large amounts of concentrated sample and potentially toxic paramagnetic quenchers. A useful optical approach to measure P_d has been to exploit the dependence of fluorescence quantum yield of certain fluorophores to H_2O/D_2O content. It was found that the fluorescence of aminonapthalene trisulfonic acid (ANTS) increases by >3-fold when H_2O is replaced by D_2O; this approach was utilized to measure P_d in liposomes and red cell membranes [86]. The time course of intravesicular ANTS fluorescence has been measured in a stopped-flow experiment in which vesicles in an H_2O-containing buffer were mixed rapidly with an isosmotic D_2O-containing buffer (Fig. 1*E*). P_d in kidney tubules has been measured by luminal perfusion of ANTS in an H_2O-containing buffer and bath perfusion with a D_2O-containing buffer [46]; luminal ANTS fluorescence at the distal end of the tubule, taken together with luminal flow and tubule geometry, provided a quantitative measure of P_d. Recently, we have found that several cell permeable and trappable SNARF/SNAFL fluorophores exhibit H_2O/D_2O-dependent quantum yields, providing a noninvasive approach to measure P_d in living cells. Alternative optical strategies that might be useful for measurement of P_d in some systems include exploiting the different refractive indices or infrared light absorbances of H_2O *vs.* D_2O.

Solute Permeability Deduced from Volume Measurements

A convenient approach to follow solute transport is to measure osmotically induced changes in vesicle or cell volume that accompany solute transport. The principle is demonstrated in Fig. 1*F*. Vesicles are subjected to an inward gradient of a solute such as urea. Because water is more permeable than urea, there is initial osmotic water efflux and cell shrinkage; as urea enters, there is water influx and swelling back to the initial volume. The light-scattering or fluorescence methods described above may be used to follow volume changes; however, it is noted that potential artifacts in light-scattering measurements occur because of refractive index changes accompanying solute transport [18]. Light-scattering and fluorescence methods have been used to measure the transport of various small solutes such as urea, glucose, and alkyl amides [18, 41, 79]. To deduce solute permeability from volume measurements, it is required that the rate of water transport exceed that of solute transport, and that sufficient solute concentrations are used to induce measurable volume changes.

When water permeability (P_f) is much greater than solute permeability (P_s) and volume changes are small, P_s is approximately equal to $(\tau S/V)^{-1}$, where τ is the time constant of a single exponential fit to the volume time course and S/V is cell or vesicle surface-to-volume ratio (cm^{-1}). In general, P_s is related to J_v (given by Eq. 1) and the solute flux from side 1 to side 2 of a membrane (J_s, mol/cm^2 sec) by the relation,

$$J_s = P_s([S_1] - [S_2]) + J_v(1 - \sigma_i)\langle S\rangle \quad (2)$$

where $[S]$ is solute concentration, σ_i is solute reflection coefficient, and $\langle S\rangle$ is the effective solute concentration in the membrane, often assumed to equal the mean value $([S_1] + [S_2])/2$. The first term in Eq. 2 describes concentration-driven solute movement and the second term describes the solvent drag of solute. Equations 1 and 2 are the Kedem-Katchalsky nonequilibrium thermodynamic equations for coupled water and solute movement [40], and can be numerically integrated for application to specific transport problems [18, 47, 59, 66]. It is noted that the solute reflection coefficient σ_i, which provides information about solute-solvent coupling through a common pathway [25], can in principal be measured from the ability of a solute gradient to induce osmotic water movement (''induced osmosis,'' Eq. 1) or from the ability of volume flux to induce solute transport (''solvent drag,'' Eq. 2). Several examples of σ_i determination are cited [47, 59, 66,] in which detailed technical considerations are discussed.

Ion and Ion-coupled Transport

The strategies to study water and neutral solute transport described in the previous section rely on measurement of the *time-integrated* outcome of a transport event (such as cell volume change in response osmotic water flow). No method exists at present to measure the *instantaneous* flow of water or neutral solutes across a membrane. For electrogenic transport of ions, or of solutes coupled to ions, transport can be measured by both ''time-integrated'' and ''instantaneous'' methods. For time-integrated measurements (such as increasing cellular $[Cl^-]$ in response to an inward Cl^- gradient), cells or vesicles are loaded with a fluorescent dye in which ion concentration is deduced from a fluorescence signal (intensity, spectral change, anisotropy, lifetime). For time-integrated ion transport measurements, ion-sensitive fluorescence indicators usually offer considerable technical advantages over radioisotope uptake or ion-sensitive microelectrode methods. However, for measurement of instantaneous ion currents, electrophysiological methods are generally superior to potential-sensitive fluorescent probes.

An ideal ion-sensitive fluorescent indicator should be loadable into cells noninvasively and remain en-

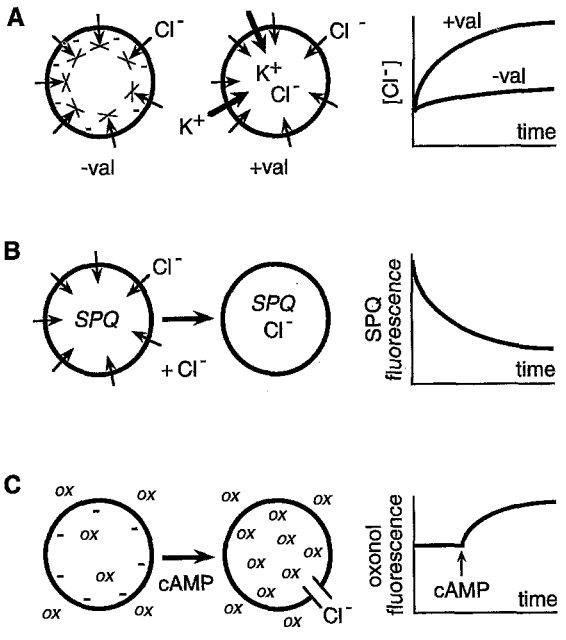

Fig. 2. Experimental strategies to measure ion transport. (*A*) Design of an ion transport measurement study in which vesicles are subjected to an inwardly directed gradient of Cl^-. Case I (–val): Cl^- provides the major conductance; Case II (+val): valinomycin has been added in the presence of K^+ so that Cl^- transport is rate-limiting. (*B*) Measurement of Cl^- transport by SPQ fluorescence. Cells loaded with SPQ and are subjected to an inward Cl^- gradient. Cl^- entry causes SPQ fluorescence quenching. (*C*) Measurement of cAMP-stimulated chloride conductance in cells by the membrane potential-sensitive probe bis-oxonol. Increased plasma membrane Cl^- conductance causes depolarization and intracellular accumulation of bis-oxonol (*ox*). *See* text for details.

trapped in the desired intracellular compartment. The indicator should not buffer the ion being studied and not interfere with cellular metabolic or transporting functions. The optical signal response to a change in ion concentration should be large and rapid, and not affected by other cellular components. For fluorescence microscopy applications, the fluorophore should be bright (high molar absorbance and quantum yield), nonphototoxic, and resistant to photobleaching. Fluorophore excitation by visible light (>420 nm) is preferred to UV excitation to minimize background instrument and cellular autofluorescence, and to minimize photodynamic cell injury. As a general guideline, the illumination intensity for cellular applications should be so low that the cells can be visualized by the unaided eye only after acclima-tion to the dark. Finally, the shape of the fluorescence excitation and/or emission spectrum of an ideal indicator should be sensitive to ion concentration, producing a fluorescence signal suitable for ratio imaging.

Quantitative analysis of ion transport involves measurement of ion movement in response to a defined electrochemical driving force. For transport of a single positively charged ion such as K^+, the flux across a membrane (J_{K^+}, mol · $cm^{-1}s^{-1}$) is given by,

$$J_{K^+} = P_{K^+}(\phi F/RT)([K^+]_1 e^{-\phi F/RT} - [K^+]_2)/(1 - e^{\phi F/RT}) \quad (3)$$

where P_{K^+} (cm/sec) is the permeability coefficient, ϕ is membrane potential (mV) and *RT/F* is ~60 mV at 37°C. Note that both ion concentrations and membrane potential must be specified to define the electrochemical gradient. Expressions similar to Eq. 3 can be written to describe more complex ion-coupled transport events, as well as ion-coupled water transport [3, 29, 35]. For time-integrated measurements, ion flux is related to the kinetics of intracellular ion concentration, taking into account any binding/titration processes (as occurs in H^+ and Ca^{++} transport). For current measurements, ion flux is related to ion conductance. As a practical consideration, ion transport measurements must be designed to insure that the transport event of interest is *rate-limiting*. For example, in studying Cl^- transport, electroneutrality requires that Cl^- movement be accompanied by cotransport of a cation or countertransport of an anion (Fig. 2*A*). Generally, an ion-ionophore pair can be provided to satisfy electroneutrality and insure that the transport event of interest is rate-limiting. Effective ionophores are available for electrogenic movement of K^+ (valinomycin) and H^+ (CCCP), and an ionophore has recently become available for Na^+; note that the compounds nigericin (K^+/H^+ exchanger), monensin (Na^+/H^+ exchanger) and tributyltin (Cl^-/OH^- exchanger) produce nonelectrogenic transport and are thus not suitable to satisfy electroneutrality.

The general principles described above are illustrated for specific examples in the measurement of anion and cation transport. The properties and limitations of ion- and membrane potential-sensitive fluorescent indicators are discussed.

Chloride Transport

The development of Cl^--sensitive fluorescent indicators has been particularly useful in cystic fibrosis research, where the defective gene encodes the CFTR Cl^- channel. It was initially found that the fluorescence of the N-substituted quinolinium indicator SPQ (6-methoxy-N-[3-sulfopropyl] quinolinium) (Fig. 3*A*) was Cl^- sensitive and selective, and that the physical properties of SPQ were potentially desirable for biological applications [36]. SPQ is a water-soluble, membrane-impermeant fluorophore with excitation and emission wavelengths of 320–370 and 430–470 nm, respectively. SPQ fluorescence is quenched by Cl^- in <1 msec by a collisional mechanism (Stern-Volmer constant of 118 M^{-1}; 50% quenching at 8 mM Cl^-), without a change in spectral shape. SPQ fluorescence is also quenched strongly by Br^-, I^-, and SCN^-, and weakly by some organic ions;

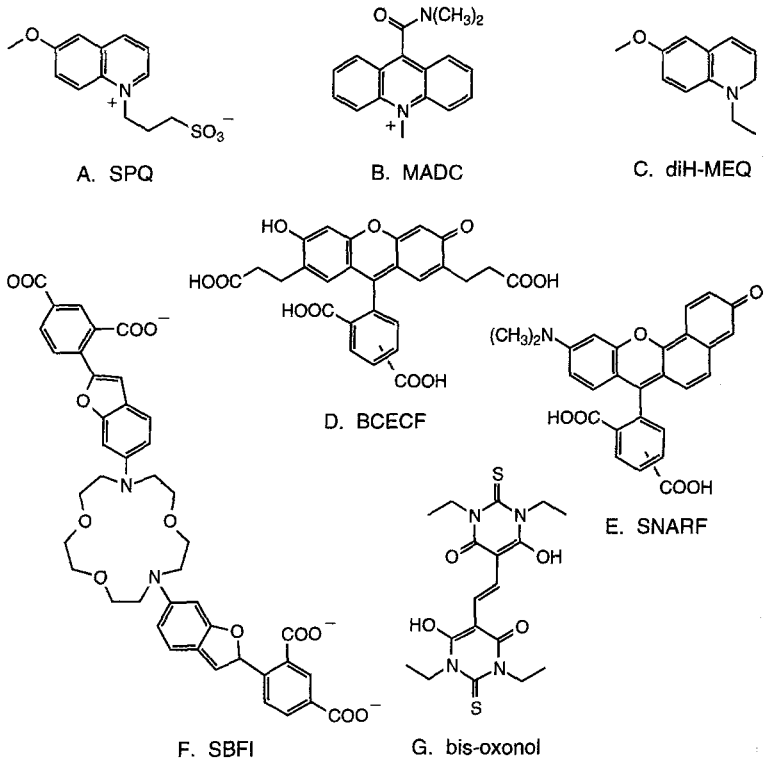

Fig. 3. Chemical structures of selected ion-sensitive fluorescent indicators.

SPQ fluorescence is not sensitive to NO_3^-, SO_4^{-2}, PO_4^{-3}, cations, pH, and ionic strength. The utility of SPQ for measurement of Cl^- transport in various cell and membrane preparations was first examined, and then tailored indicators with improved Cl^- sensitivity, optical properties, and cell loading were synthesized [74, 77].

Applications in Cells and Epithelia

An initial study was performed using fibroblasts and epithelial cells from kidney and trachea cultured on glass coverslips [14, 15]. SPQ was loaded by a hypotonic shock procedure or by overnight incubation in medium containing 1–5 mM SPQ. The loaded cells were stained brightly and uniformly with SPQ, and had similar signaling and electrical properties to cells that had not been subjected to hypotonic shock. SPQ leaked out from loaded cells at rates of 0–10%/hr at 37°C. Using low intensity illumination and sensitive detection optics, intracellular Cl^- activity could be monitored continuously for >3 hr without measurable photobleaching. Calibration of SPQ fluorescence *vs.* intracellular $[Cl^-]$ was carried out using the ionophores tributyltin and nigericin in the presence of high K^+. In tracheal epithelial cells grown on porous filters mounted in an Ussing-type perfusion chamber, an apical membrane Cl^- conductance and a basolateral membrane Na/K/2Cl symporter were characterized [78]. SPQ has been used widely in cystic fibrosis research to measure cAMP-stimulated Cl^- transport in native cells and cells transfected with wild-type and mutant CFTR [19, 20, 61].

SPQ was used to study Cl^- transport in an intact epithelia, the isolated perfused kidney proximal tubule [42]. Cells were loaded by a 15-min luminal perfusion with 20 mM SPQ at 37°C and the ionophore calibration procedure was carried out *in situ*. $[Cl^-]$ was found to be above electrochemical equilibrium, and basolateral membrane Cl^- transport was rapid, supporting the presence of a significant transcellular Cl^- flux. Measurement of the transepithelial NaCl reflection coefficient was carried out by a ratio imaging technique [66]. SPQ and fluorescein sulfonate were used as extracellular Cl^--sensitive and insensitive indicators for ratio imaging measurement of Cl^- concentration along the axis of the tubule lumen. Axial profiles obtained with zero initial luminal Cl^-, physiological bath Cl^-, and a series of transepithelial osmotic gradients were analyzed by a nonequilibrium thermodynamic model of solute-solvent transport. The transepithelial and basolateral membrane NaCl reflection coefficients did not differ significantly from unity, indicating absence of solvent drag. Recently, a Cl^--sensitive fluorescent dextran (*see below*) was used as an extracellular marker to measure Cl^- activity in the lateral intercellular space of MDCK cells [85].

Applications in Membrane Vesicles

SPQ can be loaded into isolated biomembrane vesicles by prolonged incubation (e.g., 12 hr, 4°C, 10 mM SPQ) or

by hypotonic shock (e.g., 150 mOsm, 3 min, 2 mM SPQ) [16, 59]. For liposome experiments, SPQ can be present at the time of liposome formation by sonication, detergent dialysis or extrusion [82]. External indicator is removed by centrifugation or exclusion chromatography. Cl^- influx or efflux is measured from the time course of fluorescence in response to Cl^- gradients using a fluorimeter, or when millisecond time resolution is required, using a stopped-flow apparatus (Fig. 2*B*). This approach has been used to characterize Cl^- transporters and NaCl reflection coefficient in membrane vesicles isolated from kidney and tracheal epithelia [16, 59], and to study proteoliposomes reconstituted with Cl^- channels [21, 30, 57]. SPQ has also been used to measure Cl^- transport in isolated endocytic vesicles. Because SPQ is nontoxic and membrane-impermeant, it is suitable as a marker of fluid-phase endocytosis in cell culture and intact animal studies. The strategy is to label endosomes by fluid-phase endocytosis, homogenize cells, and prepare a crude microsomal pellet containing the fluorescently-labeled endosomes. Cultured cells are labeled by inclusion of SPQ into the medium; endosomes from specific organs such as kidney cortex are labeled by intravenous infusion of SPQ. In endocytic vesicles from proximal tubule apical membrane, Cl^- transport was conductive and modulated by protein kinase A-dependent phosphorylation [4].

Structure-Activity Relationships of Cl^- Indicators

Because there were no photochemical principles to facilitate the design of Cl^- indicators, ~30 SPQ analogues with specific structural modifications were initially synthesized [43, 81]. Water solubility, strong fluorescence, and high Cl^- sensitivity required N-substituted heterocyclic compounds like SPQ. Examination of the 'backbone' moiety by synthesis of N-[3-sulfopropyl] derivatives of quinoline, isoquinoline, phenanthridine and the benzoquinolines revealed that the quinoline backbone gave by far the highest Cl^- sensitivity, whereas the 3-ringed backbones, with extended ring conjugation, gave desirable red-shifted excitation and emission spectra. Of the N-substituted quinoline derivatives, good Cl^- sensitivity and optical properties required ring substitution with a single, 'electron-donating' group (e.g., methoxy, methyl). Substitution at positions 2–6 gave acceptable compounds, whereas substitution at positions 7 and 8 with any group, or at any position with an 'electron-withdrawing' group (e.g., halide, carboxyl), resulted in loss of Cl^- sensitivity. The charge density in the vicinity of the quaternary heterocyclic nitrogen dramatically influenced Cl^- sensitivity [8]; replacement of the 3′-sulfopropyl group by 3′-aminopropyl increased Cl^- sensitivity >3-fold when the amino group was positively charged.

Synthesis of Cl^- Indicators with Improved Properties

These empirical structure-function relationships established a rational approach for the design of Cl^- indicators with improved sensitivity, optical properties and cell permeability. Alkylation of APQ to the trimethylammonium moiety gave a pH-insensitive indicator with a Cl^- sensitivity 3 times greater than that of SPQ [8]. A compound with extended conjugation, 6-phenyl-ABQ, had similar Cl^- sensitivity to SPQ, with a marked red-shifted spectrum (emission 470–490 nm). For application as a fluid-phase Cl^- indicator, Cl^--sensitive dextran conjugates were synthesized containing a second Cl^--insensitive chromophore (lucifer yellow). Based on the Cl^- sensitivity of the 9,9′-bisacridinium compound lucigenin, 9-substituted acridinium compounds were introduced as a new class of long-wavelength Cl^- indicators [9] (Fig. 3*B*). Four compounds were synthesized with ~3 times more Cl^- sensitivity than SPQ, and bright green fluorescence with peak emission wavelengths up to 530 nm. The acridinium indicators were used to measure Cl^- transport in biomembrane vesicles and proteoliposomes reconstituted with Cl^- channels, but were not suitable for measurement of cytosolic Cl^- because they were converted to a Cl^--insensitive product in the cytoplasm (by addition of an OH^- group at the 9 position). Last, a cell-permeable compound was synthesized which is metabolically converted to a Cl^--sensitive indicator which remains entrapped in cells. diH-MEQ (Fig. 3*C*) is a reduced 1,2-dihydroquinoline that is membrane permeable and readily oxidized in cell cytosol to the impermeable, fluorescent, and Cl^--sensitive compound 6-methoxy-N-ethylquinolinium (MEQ) [10]. diH-MEQ was applied successfully to measure regulated Cl^- transport in various cell systems, such as kinin-induced Cl^- efflux in epithelial cells [51].

Transport of Protons and Cations

Proton Transport

Proton movement across membranes is readily measured from pH changes as intravesicular or intracellular buffers are titrated [50, 72]. A number of excellent fluorescent pH indicators have been utilized to measure active and passive electrogenic H^+ transport, and electroneutral H^+ transport processes such as Na^+/H^+ and Cl^-/OH^- antiport. Fluoresceins have been most widely used as pH indicators. Several fluorescein derivatives are available with pKa's between 5 and 7 and with pH-dependent fluorescence excitation spectra. Fluorescein-labeled dextrans and pyranine (pKa ~ 7.5) are good membrane-impermeant pH indicators [31, 32]. The multivalent fluorescein derivative BCECF (Fig. 3*D*) (pKa ~ 7) has been used extensively to measure intracellular pH; BCECF-

acetoxymethyl ester is cell permeable and cleaved by cytosolic esterases to the membrane-impermeant BCECF [69]. Newer dyes of the benzoxanthene class, SNARF (Fig. 3*E*) and SNAFL, have pKas of 7–7.6 and permit pH measurement by excitation or emission ratio imaging [83]. The coumarin and rhodol chromophores are also useful for measurement of pH when conjugated to suitable substrates.

Sodium and Potassium Transport

Fluorescent indicators for Na^+ and K^+ have recently became available. SBFI (for Na^+) (Fig. 3*F*) and PBFI (for K^+) are UV-excitable dyes suitable for excitation ratio imaging [54]. Measurements of cation concentrations with these dyes however are quite challenging because of their low quantum yields and imperfect Na^+ *vs.* K^+ selectivities. The K_d for SBFI increases from ~10 to 20 mM Na^+ as K^+ increases from 0 to physiological intracellular levels; PBFI has little selectivity for K^+ over Na^+, requiring difficult calibration procedures. SBFI has been used to measure Na^+ concentrations in a number of different cell types (e.g., *refs.* 11, 33, 55, 58). A long-wavelength Na^+ indicator was introduced recently (Sodium Green™, Molecular Probes), with a reported increase in fluorescence upon Na^+ binding with a K_d of 6 mM.

Other Cations

Indicators to measure the transport of other cations are mentioned briefly. There is an extensive body of literature on the application of Ca^{++} indicators to study intracellular signaling. These indicators (fura-2, indo-1) and their long-wavelength counterparts (fluo-3, rhod-2, Calcium Green™) are suitable for Ca^{++} transport studies [53]. Various relatively Ca^{++}-insensitive analogues of these compounds (e.g., mag-fura-2) have been used as Mg^{++} indicators because the concentration of ionized Mg^{++} in cells is much greater than that of Ca^{++} [38]. Recently, compounds have been identified that may serve as indicators of Zn and the heavy metals Cd, Hg, Pb and Ba [29], although the biological utility of these indicators has not been established.

Membrane Potential-sensitive Probes

Measurement of membrane potential provides key information in the study of conductive transport processes. Several classes of membrane potential-sensitive fluorescent dyes have been developed. Carbocyanines are positively-charged "slow" dyes that accumulate in negative compartments [13]. Although carbocyanines are not suited for measurements in intact cells because of accumulation in mitochondria and binding to intracellular components, they are useful for potential measurements in membrane vesicles, liposomes and mitochondria [60, 62, 84]. Signal changes are relatively large, and calibration of carbocyanine fluorescence *vs.* potential can be accomplished by generation of K^+/valinomycin diffusion potentials. The styryl class of lipophilic dyes respond very fast to changes in membrane potential by an electrochromic mechanism, defined as a nearly instantaneous change in electronic configuration [48]. The major difficulty with these dyes is their low sensitivity to membrane potential (<10% signal change per 100 mV), restricting measurements to electrically excitable cells in which repetitive stimulation and signal averaging are possible, although applications in other cell types may be feasible [49]. The merocyanine class of dyes, which respond to membrane potential by a membrane accumulation-re-orientation mechanism [71], are very photosensitive, and like the styryl dyes, have low sensitivity to changes in membrane potential.

Dyes of the oxonol class (including bis-oxonol, Fig. 3*G*) have been used to measure membrane potential in intact cells. Oxonals are negatively charged dyes that accumulate slowly (seconds to minutes) in depolarized intracellular compartments. There is a measurable fluorescence enhancement as oxonols accumulate and bind to various intracellular components (Fig. 2*C*). Compared to the carbocyanine and merocyanine classes, oxonols are less toxic to cells; however, their slow response and sensitivity to potential independent factors (such as intracellular composition) make quantitative membrane potential measurements difficult. Oxonals have been applied to measure membrane potential changes in a variety of cellular systems (e.g., *refs.* 52, 63).

Future Directions

With continued improvements in instrument technology and indicators, optical methods are likely to play an increasingly important role in quantifying membrane transport phenomena. The development of new chromophores should permit the wider use of fluorescently tagged substrates to measure substrate transport. For example, fluorescein has been used as a marker for organic ion transport, and fluorescently labeled fatty acids and oligopeptides have been used to measure lipid and protein transport [68]. The possibility of utilizing intrinsic cellular fluorescence as an indicator of pH and ion concentration is intriguing. For example, modifications of the green fluorescent protein may permit ion sensing in targeted subcellular compartments.

New techniques such as single photon radioluminescence (SPR) may provide generic detection methods for transport processes [7]. SPR arises from the excitation of a fluorophore by the energy deposited from a beta decay electron. This phenomenon has been exploited to

measure ^{3}H-glucose influx into BCECF-loaded cells from the increasing SPR signal that arises when ^{3}H-glucose and BCECF are in close proximity [54]. Detection of indicator fluorescence by near field microscopy might permit the study of solute flow very near specific transporting site in membranes. New methods to measure osmotic water transport in intact epithelia and tissues are required to evaluate the physiological role of water channels; strategies utilizing laser interferometry and flow-dependent fluorescence quenching are under development in the laboratory. Optical methods are also ideal to address relatively unexplored questions about the ionic content, membrane potential and transport characteristics of intracellular organelles. Aqueous-phase indicators can be loaded into endosomes and mitochondria, and a novel liposome-injection procedure permits the introduction of fluorescent indicators selectively into the *trans*-Golgi compartment [64]. Lipid-indicator constructs, such as the lipophilic Ca^{++} indicator fura-indoline-C_{18} [23], should provide insight into the unique milieu of membrane-adjacent cytoplasm.

There are a number of improvements which should extend remarkably the usefulness of existing methods. Cation indicators with improved optical properties are needed for studies of Na^+ and K^+ transport. A cell-loadable Cl^- indicator with a Cl^--dependent spectral shift is required to map absolute Cl^- activity in living cells. Improvements in sensitivity and specificity are needed in existing membrane potential-sensitive indicators for use in living cells. Last, there is a need for new classes of indicators for detection of intracellular components such as phosphate, where adequate alternative measurement methods do not exist.

I thank Joachim Biwersi, Javier Farinas and Nallagounder Periasamy for critical review of this manuscript. This work was supported by grants DK43840, DK35124, HL42368 and HL85854 from the National Institutes of Health, and grants from the National Cystic Fibrosis Foundation and American Heart Association.

References

1. Agre, P., Preston, G., Smith, B., Jung, S., Raina, C., Moon, W., Guggino, W., Nielsen, S. 1993. Aquaporin CHIP: the archetypal molecular water channel. *Am. J. Physiol.* **265:**F463–F476
2. Al-Zahid, B., Schafer, J.A., Troutman, S.L., Andreoli, T.E. 1977. Effect of antidiuretic hormone on water and solute permeation, and the activation energies of these processes in mammalian cortical collecting tubules. *J. Membrane Biol.* **31:**103–129
3. Andreoli, T.E., Hoffman, J.F., Fanestil, D.D., Schultz, S.G. 1986. Physiology of Membrane Disorders. Plenum Press, New York
4. Bae, H.-R., Verkman, A.S. 1990. Protein kinase A regulates chloride conductance in endocytic vesicles from proximal tubule. *Nature* **348:**635–637
5. Barry, P.H., Diamond, J.M. 1984. Effects of unstirred layers on membrane phenomena. *Physiol. Rev.* **64:**763–872
6. Bicknese, S., Periasamy, N., Shohet, S.B., Verkman, A.S. 1993. Cytoplasmic viscosity near the cell plasma membrane: measurement by evanescent field frequency-domain microfluorimetry. *Biophys. J.* **65:**1272–1282
7. Bicknese, S., Shahrohk, Z., Shohet, S.B., Verkman, A.S. 1992. Single photon radioluminescence. I. Theory and spectroscopic properties. *Biophys. J.* **63:**1256–1266
8. Biwersi, J., Farah, N., Wang, Y.-X., Ketchum, R., Verkman, A.S. 1992. Synthesis of cell-impermeable Cl-sensitive fluorescent indicators with improved sensitivity and optical properties. *Am. J. Physiol.* **262:**C243–C250
9. Biwersi, J., Tulk, B., Verkman, A.S. 1994. Long wavelength chloride-sensitive fluorescent indicators. *Anal. Biochem.* **219:**139–143
10. Biwersi, J., Verkman, A.S. 1991. Cell permeable fluorescent indicator for cytosolic chloride. *Biochemistry* **30:**7879–7883
11. Borle, A.B., Bender, C. 1991. Effects of pH on Ca_i^{2+}, Na_i^+, and pH_i of MDCK cells: Na^+-Ca^{2+} and Na^+-H^+ antiporter interactions. *Am. J. Physiol.* **261:**C482–C489
12. Brahm, J. Diffusional water permeability of human erythrocytes and their ghosts. *J. Gen. Physiol.* **79:**791–819
13. Cabrini, G., Verkman, A.S. 1986. Potential sensitive response mechanism of diS-C_3-(5) in biological membranes. *J. Membrane Biol.* **92:**171–182
14. Chao, A.C., Dix, J.A., Sellers, M., Verkman, A.S. 1989. Fluorescence measurement of chloride transport in monolayer cultured cells: mechanisms of chloride transport in fibroblasts. *Biophys. J.* **56:**1071–1081
15. Chao, A.C., Widdicombe, J.H., Verkman, A.S. 1990. Chloride transport mechanisms in cultured canine tracheal epithelial cells measured by an entrapped fluorescent indicator. *J. Membrane Biol.* **113:**193–202
16. Chen, P.-Y., Illsley, N.P., Verkman, A.S. 1988. Renal brush border chloride transport mechanisms characterized using a fluorescent indicator. *Am. J. Physiol.* **254:**F114–F120
17. Chen, P-Y., Pearce, D., Verkman, A.S. 1988. Membrane water and solute permeability determined quantitatively by self-quenching of an entrapped fluorophore. *Biochemistry* **27:**5713–5719
18. Chen, P.-Y., Verkman, A.S. 1987. Nonelectrolyte transport across renal proximal tubule cell membranes measured by tracer efflux and light scattering. *Pfluegers Arch.* **408:**491–496
19. Cheng, S.H., Rich, D.P., Marshall, J., Gregory, R.J., Welsh, M.J., Smith, A.E. 1991. Phosphorylation of the R domain by cAMP-dependent protein kinase regulates the CFTR chloride channel. *Cell* **66:**1027–36
20. Dho, S., Foskett, J.K. 1993. Optical imaging of Cl-permeabilities in normal and CFTR-expressing mouse L cells. *Biochim. Biophys. Acta* **1152:**83–90
21. Dunn, S.M.J., Martin, C. Agey, M.W., Miyazaki, R. 1989. Functional reconstitution of the bovine brain GABA receptor from solubilized components. *Biochemistry* **28:**2545–2551
22. Echevarria, M., Verkman, A.S. 1992. Optical measurement of osmotic water transport in cultured cells: evaluation of the role of glucose transporters. *J. Gen. Physiol.* **99:**573–589
23. Etter, E.F., Kuhn, M.A., Fay, F.S. 1994. Detection of changes in near-membrane Ca^{2+} concentration using a novel membrane associated with Ca^{2+} indicator. *J. Biol. Chem.* **269:**10141–10149
24. Farinas, J., Simenak, V., Verkman, A.S. 1995. Cell volume measured in adherent cells by total internal reflection microfluorimetry: application to permeability in cells transfected with water channel homologs. *Biophys. J.* **68:**1613–1620
25. Finkelstein, A. 1987. Water Movement through Lipid Bilayers, Pores, and Plasma Membranes: Theory and Reality. New York, Wiley & Sons
26. Fischbarg, J., Kunyan, K., Hirsch, J., Lecuona, S., Rogozinski, L., Silverstein, S., Loike, J. 1989. Evidence that the glucose trans-

porter serves as a water channel in J774 macrophages. *Proc. Natl. Acad. Sci. USA* **86:**8397–8401
27. Fischbarg, J., Kunyan, K., Vera, J.C., Arant, S., Silverstein, S., Loike, J., Rosen, O.M. 1990. Glucose transporters serve as water channels. *Proc. Natl. Acad. Sci. USA* **87:**3244–3247
28. Flamion, B., Spring, K.R. 1990. Water permeability of apical and basolateral cell membranes of rat inner medullary collecting duct. *Am. J. Physiol.* **259:**F986–F999
29. Frederickson, C.J., Kasarskis, E.J., Ringo, D., Frederickson, R.E. 1987. A quinoline fluorescence method for visualizing and assaying the histochemically reactive zinc (Bouton zinc) in the brain. *J. Neurosci. Meth.* **20:**91–103
30. Garcia-Calvo, M., Ruiz-Gomez, A., Vazquez, J., Morato, E., Valdivieso, R., Mayor, F. 1989. Functional reconstitution of the glycine receptor. *Biochemistry* **28:**6405–6409
31. Giuliano, K., Gillies, R. 1987. Determination of intracellular pH of BALB/c-3T3 cells using fluorescence of pyranine. *Anal. Biochem.* **167:**362–371
32. Graber, M.L., DiLillo, D.C., Friedman, B.L., Pastoriza, E., Munoz, E. 1986. Characteristics of fluoroprobes for measuring intracellular pH. *Anal. Biochem.* **156:**202–212
33. Harootunian, A.T., Kao, J.P., Eckert, B.K., Tsien, R.Y. 1989. Fluorescence ratio imaging of cytosolic free Na^+ in individual fibroblasts and lymphocytes. *J. Biol. Chem.* **264:**19458–19467
34. Harris, H. W., Handler, J.S., Blumenthal, R. 1990. Apical membrane vesicles of ADH-stimulated toad bladder are highly water permeable. *Am. J. Physiol.* **258:**F237–F243
35. Hartmann, T., Verkman, A.S. 1990. Model of ion transport regulation in chloride-secreting airway epithelial cells: integrated description of electrical, chemical and fluorescence measurements. *Biophys. J.* **58:**391–401
36. Illsley, N.P., Verkman, A.S. 1987. Membrane chloride transport measured using a chloride-sensitive fluorescent indicator. *Biochemistry* **26:**1215–1219
37. Jiang, C., Finkbeiner, W.E., Widdicombe, J.H., McCray, P.B., Jr., Miller, S.S. Altered fluid transport across airway epithelium in cystic fibrosis. *Science* **262:**424–427
38. Jung, D.W., Apel, L., Brierley, G.P. 1990. Matrix free Mg^{2+} changes with metabolic state in isolated heart mitochondria. *Biochemistry* **29:**4121–4128
39. Kao, H.P., Verkman, A.S. 1994. Tracking of single fluorescent particles in three dimensions: use of cylindrical optics to encode particle position. *Biophys. J.* **67:**1291–1300
40. Kedem, O., Katchalsky, A. 1958. Thermodynamic analysis of the permeability of biological membranes to nonelectrolytes. *Biochim. Biophys. Acta* **27:**229–246
41. Kim, Y., Illsley, N.P., Verkman, A.S. 1988. Rapid fluorescence assay of glucose and neutral solute transport using an entrapped volume indicator. *Anal. Biochem.* **172:**403–409
42. Krapf, R., Berry, C.A., Verkman, A.S. 1988. Estimation of intracellular chloride activity in isolated perfused rabbit proximal tubules using a fluorescent probe. *Biophys. J.* **53:**955–962
43. Krapf, R., Illsley, N.P., Tseng, H.C., Verkman, A.S. 1988. Structure-activity relationships of chloride-sensitive fluorescent indicators for biological application. *Anal. Biochem.* **169:**142–150
44. Kuwahara, M., Berry, C.A., Verkman, A.S. 1988. Rapid development of vasopressin-induced hydroosmosis in kidney collecting tubules measured by a new fluorescence technique. *Biophys. J.* **54:**595–602
45. Kuwahara, M., Shi, L.-B., Marumo, F., Verkman, A.S. 1991. Transcellular water flow modulates water channel exocytosis and endocytosis in kidney collecting tubule. *J. Clin. Invest.* **88:**423–429
46. Kuwahara, M., Verkman, A.S. 1988. Direct fluorescence measurement of diffusional water permeability in the vasopressin-sensitive kidney collecting tubule. *Biophys. J.* **54:**587–593
47. Levitt, D.G., Mlekoday, H.J. 1983. Reflection coefficient and permeability of urea and ethyleneglycol in the human red cell membrane. *J. Gen. Physiol.* **81:**239–254
48. Loew, L.M. 1992. Voltage-sensitive dyes: measurement of membrane potentials induced by DC and AC electric fields. *Bioelectromag. Suppl.* **1:**179–189
49. Loew, L.M., Cohen, L.B., Dix, J., Fluhler, E.N., Montana, V., Salama, G., Wu, J.Y. 1992. A naphthyl analog of the aminostyryl pyridinium class of potentiometric membrane dyes shows consistent sensitivity in a variety of tissue, cell, and model membrane preparations. *J. Membrane Biol.* **130:**1–10
50. Lukacs, G.L., Kapus, A., Nanda, A., Romanek, R., Grinstein, S. 1993. Proton conductance of the plasma membrane: properties, regulation, and functional role. *Am. J. Physiol.* **265:**C3–C14
51. MacVinish, L.J., Reancharoen, T., Cuthbert, A.W. 1993. Kinin-induced chloride permeability changes in colony 29 epithelia estimated from ^{125}I efflux and MEQ fluorescence. *Brit. J. Pharm.* **108:**469–478
52. Mason, M.J., Grinstein, S. 1990. Effect of cytoplasmic acidification on the membrane potential of T-lymphocytes: role of trace metals. *J. Membrane Biol.* **116:**139–148
53. Minta, A., Kao, J., Tsien, R. 1989. Fluorescent indicators for cytosolic calcium based on rhodamine and fluorescein chromophores. *J. Biol. Chem.* **264:**8171–8178
54. Minta, A., Tsien, R.Y. 1989. Fluorescent indicators for cytosolic sodium. *J. Biol. Chem.* **264:**19449–19457
55. Moore, E.D., Fay, F.S. 1993. Isoproterenol stimulates rapid extrusion of sodium from isolated smooth muscle cells. *Proc. Natl. Acad. Sci. USA* **90:**8058–8062
56. Muallem, S., Zhang, R., Loessberg, P.A., Star, R.A. 1992. Simultaneous recording of cell volume changes and intracellular pH or Ca^{2+} concentration in single osteosarcoma cells UMR-106-01. *J. Biol. Chem.* **267:**17658–17664
57. Mulberg, A.E., Tulk, B.M., Forgac, M. 1991. Modulation of coated vesicle chloride channel activity and acidification by reversible protein kinase A-dependent phosphorylation. *J. Biol. Chem.* **266:**20590–20593
58. Negulescu, P.A., Machen, T.E. 1990. Intracellular ion activities and membrane transport in parietal cells measured with fluorescent dyes. *Meth. Enzymol.* **192:**38–81
59. Pearce, D., Verkman, A.S. 1989. NaCl reflection coefficients in proximal tubule apical and basolateral membrane vesicles: measurement by induced osmosis and solvent drag. *Biophys. J.* **55:**1251–1259
60. Plasek, J., Dale, R.E., Sigler, K., Laskay, G. 1994. Transmembrane potentials in cells: a diS-C3(3) assay for relative potentials as an indicator of real changes. *Biochim. Biophys. Acta* **1196:**181–190
61. Ram, S.J., Kirk, K.L. 1989. Cl permeability of human sweat duct cells monitored with fluorescence-digital imaging microscopy: evidence for reduced plasma membrane Cl permeability in cystic fibrosis. *Proc. Natl. Acad. Sci. USA* **24:**10166–10170
62. Reers, M., Smith, T.W., Chen, L.B. 1991. J-aggregate formation of a carbocyanine as a quantitative fluorescent indicator of membrane potential. *Biochemistry* **30:**4480–4486
63. Seamer, L.C., Mendler, R.N. 1992. Method to improve the sensitivity of flow cytometric membrane potential measurements in mouse spinal cord cells. *Cytometry* **13:**545–552
64. Seksek, O., Biwersi, J., Verkman, A.S. 1995. Direct measurement of *trans*-Golgi pH in living cells and regulation by second messengers. *J. Biol. Chem.* **270:**4967–4970
65. Shahrohk, Z., Bicknese, S., Shohet, S.B., Verkman, A.S. 1992.

Single photon radioluminescence. II. Experimental detection and biological applications. *Biophys. J.* **63:**1267–1279

66. Shi, L.-B., Fushimi, K., Verkman, A.S. 1991. Solvent drag measurement of transcellular and basolateral membrane NaCl reflection coefficient in mammalian proximal tubule. *J. Gen. Physiol.* **98:**379–398
67. Shi, L.-B., Verkman, A.S. 1989. Very high water permeability in vasopressin-dependent endocytic vesicles in toad urinary bladder. *J. Gen. Physiol.* **94:**1101–1115
68. Sullivan, L.P., Grantham, J.A., Rome, L., Wallace, D., Grantham, J.J. 1990. Fluorescein transport in isolated proximal tubules *in vitro:* epifluorometric analysis. *Am. J. Physiol.* **258:**F46–F51
69. Thomas, J.A., Buchsbaum, R.N., Zimniak, A., Racker, E. 1979. Intracellular pH measurements in Ehrlich ascites tumor cells utilizing spectroscopic probes generated *in situ. Biochemistry* **18:**2210–2218
70. Van Hoek, A.N., Verkman, A.S. 1992. Functional reconstitution of the isolated erythrocyte water channel CHIP28. *J. Biol. Chem.* **267:**18267–18269
71. Verkman, A.S. 1987. Mechanism and kinetics of merocyanine 540 binding to phospholipid membranes. *Biochemistry* **26:**4050–4056
72. Verkman, A.S. 1987. Passive H^+/OH^- permeability in epithelial brush border membranes. *J. Bioenerg. Biomembr.* **19:**481–493
73. Verkman, A.S. 1989. Mechanisms and regulation of water permeability in renal epithelia. *Am. J. Physiol.* **257:**C837–C850
74. Verkman, A.S. 1990. Development and biological applications of chloride-sensitive fluorescent indicators. *Am. J. Physiol.* **259:** C375–C388
75. Verkman, A.S. 1993. Water Channels. *In:* Molecular Biology Intelligence Series. pp. 1–18. R.G. Landes, Austin, Texas
76. Verkman, A.S. 1995. Molecular Biophysics of Kidney Water Channels. *In:* Molecular Biology of the Kidney in Health and Disease. D. Schlondorff and J.V. Bonventre, editors. pp. 459–468. Marcel Dekker, New York
77. Verkman, A.S., Biwersi, J. 1995. Chloride-sensitive Fluorescent Indicators. *In:* Methods in Neurosciences. vol. 27 J. Kraicer and S.J. Dixon, editors. pp. 328–339. Academic Press
78. Verkman, A.S., Chao, A.C., Hartmann, T. 1992. Hormonal regulation of chloride conductance in cultured polar airway cells measured by a fluorescent indicator. *Am. J. Physiol.* **262:**C23–C31
79. Verkman, A.S., Dix, J.A., Seifter, J.L. 1985. Water and urea transport in renal microvillus membrane vesicles. *Am. J. Physiol.* **248:**F650–F655
80. Verkman, A.S., Lencer, W., Brown, D., Ausiello, D.A. 1988. Endosomes from kidney collecting tubule contain the vasopressin-sensitive water channel. *Nature* **333:**268–269
81. Verkman, A.S., Sellers, M., Chao, A.C., Leung, T., Ketcham, R. 1989. Synthesis and characterization of improved chloride-sensitive fluorescent indicators for biological applications. *Anal. Biochem.* **178:**355–361
82. Verkman, A.S., Takla, R., Sefton, B., Basbaum, C., Widdicombe, J.H. 1989. Quantitative fluorescence measurement of chloride transport in phospholipid vesicles. *Biochemistry* **28:**4240–4244
83. Whitaker, J.E., Haugland, R.P., Prendergast, F.G. 1991. Spectral and photophysical studies of benzo[c]xanthene dyes: dual emission of pH sensors. *Anal. Biochem.* **194:**330–344
84. Wilson, H.A., Seligman, B.E., Chused, T.M. 1985. Voltage-sensitive cyanine dye fluorescence signals in lymphocytes: plasma membrane and mitochondrial components. *J. Cell Biol.* **125:**61–71
85. Xia, P., Persson, B.-E., Spring, K.R. 1995. The chloride concentration in the lateral intercellular space of MDCK cell monolayers. *J. Membrane Biol.* **144:**21–30
86. Ye, R., Verkman, A.S. 1989. Osmotic and diffusional water permeability measured simultaneously in cells and liposomes. *Biochemistry* **28:**824–829
87. Zhang, R., Logee, K., Verkman, A.S. 1990. Expression of mRNA coding for kidney and red cell water channels in *Xenopus* oocytes. *J. Biol. Chem.* **265:**15375–15378